Exothermic Effects Observed upon Heating of β_2-Microglobulin Monomers in the Presence of Amyloid Seeds†

Kenji Sasahara,‡ Hironobu Naiki,§ and Yuji Goto*,‡

Institute for Protein Research, Osaka University and CREST, Japan Science and Technology Agency, Yamadaoka 3-2, Suita, Osaka 565-0871, Japan, and Faculty of Medical Sciences, University of Fukui and CREST, Japan Science and Technology Agency, Matsuoka, Fukui 910-1193, Japan

Received April 6, 2006; Revised Manuscript Received May 30, 2006

ABSTRACT: To understand the initial stages in the formation of amyloid fibrils of β_2-microglobulin, a protein responsible for dialysis-related amyloidosis, the effects of heat on the acid-unfolded monomer at pH 2.5 were studied. In the presence of a low concentration of seed fibrils, differential scanning calorimetric thermograms of acid-unfolded β_2-microglobulin monomers showed a large decrease in heat capacity with a sigmoidal temperature-dependence, which was subsequently released at higher temperature. Measurements of circular dichroism, atomic force microscopy, ultracentrifugation, and repeated differential scanning calorimetry indicated that the exothermic sigmoidal transition is accompanied by the conversion of about 12% of the monomeric β_2-microglobulin molecules into amyloid fibrils, which subsequently dissociate into monomers at high temperature. Interestingly, amyloid fibrils, formed partly after the sigmoidal transition, exhibited a heating rate-dependent, kinetically controlled thermal response, indicating that 12% of the total protein is enough to exhibit the unique thermal response. On the other hand, the salt-induced protofibrils did not show such a calorimetric response, indicating that the kinetic thermal response is unique to the particular structure of fibrils. Taken together, although the calorimetric behavior of amyloid fibrils remains elusive, it may be interpreted in terms of the effects of heat associated with the formation, the association, and the unfolding of fibrils, in which the interactions between specific β-sheet structures and water molecules play a crucial role and are sensitively reflected in the heat capacity change in protein solution.

The specific self-association of proteins to form amyloid fibrils with a cross-β-sheet structure is now recognized as a phenomenon common to many proteins, the sequences and native structures of which can vary extensively, suggesting that there exists a general principle for their assembly (*1*−*7*). Research over the past few years has revealed how the amyloid fibril structure is stabilized by the hydrogen bond network in the extended intermolecular β-sheet architecture of peptide backbones as well as specific side-chain interactions (*4*−*7*). On the other hand, a nucleation-growth mechanism has been proposed to explain the formation of amyloid fibrils, in which non-native forms of precursor proteins slowly associate to form a nucleus, which then grows through the sequential incorporation of precursor molecules (*8*, *9*). A distinctive feature of the nucleation-growth mechanism is a lag period followed by a rapid extension reaction; the formation of the nucleus is usually thermodynamically unfavorable, while the subsequent extension is favorable. A considerable body of experimental evidence suggests that partial unfolding of the native conformation is a prerequisite for the assembly of highly ordered amyloid fibrils (*10*). However, it is still not clear how such partially unfolded molecules associate; knowledge about the formation of a nucleus, particularly the nature of the structural fluctuation that triggers the association of polypeptide chains leading to the oligomeric nucleus, is still limited (*11*−*14*). Furthermore, little is known about the thermodynamic aspects underlying the formation of amyloid fibrils.

β_2-Microglobulin (β2-m),[1] a 99-residue protein with a seven-stranded β-sandwich fold organized into two β-sheets linked by a single disulfide bond, constitutes the light chain of the major histocompatibility complex class I (*15*). β2-m is also a major component of the amyloid deposits found in patients with dialysis-related amyloidsis (*16*). This protein easily forms mature amyloid fibrils with a well-ordered, needlelike morphology in vitro by a seed-dependent extension reaction at a low pH, which renders it a suitable model system for investigating the mechanism of amyloid fibril formation (*9*, *17*−*29*). From the enthalpy and heat capacity changes of fibrillation and the effects of hydrostatic pressure on fibrils, unique structural features were suggested compared to the native structure of the same polypeptide chain: a lower level of overall internal packing associated with the possible

† This work was supported by Takeda Science Foundation and by Grants-in-Aid for Priority Areas (15076206) from the Japanese Ministry of Education, Culture, Sports, Science and Technology.

* To whom correspondence should be addressed. Prof. Yuji Goto, Institute for Protein Research, Osaka University, Yamadaoka 3-2, Suita, Osaka 565-0871, Japan. Tel, 81-6-6879-8614; fax, 81-6-6879-8616; e-mail, ygoto@protein.osaka-u.ac.jp.

‡ IPR, Osaka University.

§ University of Fukui.

[1] Abbreviations: β2-m, β_2-microglobulin; DSC, differential scanning calorimeter; CD, circular dichroism; $C_{p,app}$, apparent heat capacity; ThT, thioflavin T.

10.1021/bi0606748 CCC: $33.50
Published on Web 06/30/2006

presence of unfavorable side-chain contributions and a similar degree of surface burial within the supramolecular architecture of amyloid fibrils (*27*, *28*). The native fold has been acquired through an evolutional process pursuing the three-dimensional packing of side chains to function in vivo. However, in the main chain-dominated amyloid structure organized by cross-β-sheets, the amino acid side chains inside the fibrils are packed in a different manner from that in the native fold. Consequently, a characteristic hydration pattern, which is different from that of the native fold, might be induced due to the unique arrangement of polar and nonpolar residues on a fibril surface made of layers of protofibrils (*30*−*33*). A tube-like β-helical structure with an extensive hydrogen bond network, although its validity is still controversial, is also likely to exhibit another type of unique arrangement of polar and nonpolar residues (*34*).

In a previous study (*35*), we demonstrated the kinetically controlled thermal response of mature amyloid fibrils of β2-m and amyloid β-peptides by measuring the heat capacity of amyloid fibril solutions. The objective of the present study is to clarify the calorimetric properties of the protein in the initial stages of amyloid fibril formation. We found that moderate heat treatment of β2-m in the presence of seed fibrils results in an exothermic sigmoidal transition leading to a conformational state with calorimetric properties similar to those of mature amyloid fibrils. The results suggest that, although a detailed understanding of the response of amyloid fibrils to heat remains elusive, they can be interpreted by separating the processes into the formation, association, and unfolding of fibrils.

MATERIALS AND METHODS

Formation of Amyloid Fibrils of β2-m. Recombinant human β2-m was expressed in *Escherichia coli* and purified as described previously (*20*). Mature amyloid fibrils were formed via a seed-dependent extension reaction, in which acid-unfolded β2-m (0.1∼0.3 mg/mL) in a polymerizing buffer (50 mM sodium citrate and 100 mM NaCl, pH 2.5) was incubated overnight at 37 °C with the seed fibrils (final concentration: 5 μg/mL) (*9*, *20*, *27*). The seed fibrils were prepared by the repeated extension reaction at pH 2.5 of purified β2-m fibrils from patients and fragmented by sonication before use (*9*, *20*, *27*). Almost all the β2-m molecules were converted to mature amyloid fibrils under these conditions (*27*). The fibrils induced to form by salt (salt-induced fibrils) were prepared in a polymerizing buffer containing 0.5 M NaCl at 37 °C and pH 2.5 overnight without the seed fibrils (*17*). Protein concentrations were determined spectrophotometrically at 280 nm using an extinction coefficient of 1.63 mL mg^{-1} cm^{-1} (*20*).

Heat Treatment of β2-m Solutions. Acid-unfolded β2-m (30∼300 μg/mL) was mixed with the seed fibrils (final concentration: 0.5 μg/mL) in the polymerizing buffer at pH 2.5. The freshly mixed sample was immediately used in the heating experiments for the DSC, light scattering, ThT fluorescence, and CD measurements. For the experiments using atomic force microscopy (AFM), ultracentrifugation, and the seed-dependent extension reaction, the freshly mixed sample was heated at 60 °C/h to 68 °C and cooled in a thermostat.

Calorimetric Measurements. The heat capacity of the fibril (or protein) solutions was recorded using a Microcal VP-DSC calorimeter (Northampton, MA), as described in a previous paper (*35*). The degassed sample and matching buffer (i.e., the polymerizing buffer) solutions at pH 2.5 were carefully loaded into the calorimetric cells, which were kept under an excess pressure of 25 psi to prevent degassing during the heating. After a background scan with the buffer solution was subtracted from the scan of the sample and buffer solution, the apparent heat capacity ($C_{p,app}$) corresponding to the whole sample solution was recorded using Origin software (Microcal, Inc.). Details regarding the rate of heating and the range of temperatures are specified in the figures or figure captions.

Light Scattering and ThT Fluorescence Measurements. Light scattering and ThT fluorescence were monitored with a Hitachi F4500 fluorescence spectrometer using a quartz cell with a light path of 10 mm, in which the slit length was 2.5 nm. For light scattering, the wavelengths for excitation and emission were both set at 350 nm. For ThT fluorescence, the intensity at 485 nm with an excitation wavelength of 445 nm was monitored. The temperature of the sample solutions was controlled by circulating water from a thermostat.

CD Measurements. Measurements of circular dichroism (CD) were carried out in an AVIV model 205s spectropolarimeter using a quartz cell with a path length of 1 mm. CD spectra of β2-m at various stages of fibrillation were recorded between 250 and 200 nm, with a step size of 1 nm and an average time of 30 s. The temperature surrounding the cell was maintained at 20 ± 0.1 °C by a thermoelectrically controlled cell holder equipped to the polarimeter.

AFM Measurements. The sample solution was diluted 5-fold with water. Then, an aliquot (20 μL) of the diluted solution was spotted onto freshly cleaved mica and incubated for 1 min. Excess sample solution was blown off with compressed air. AFM images were obtained using a Nano Scope IIIa (Digital Instruments). The scanning tip was a phosphorus (*n*)-doped Si. The scan rate was 0.5 Hz.

Ultracentrifugation Measurements. Sedimentation velocity data were obtained using a Beckman-Coulter Optima XL-I analytical ultracentrifuge with an An-60 rotor and two-channel, charcoal-filled Epon cells at 4.0 °C. The samples were 0.2 mg/mL of β2-m in the absence or presence of 0.5 μg/mL of seed fibrils, and the polymerizing buffer was used. The sedimentation velocity experiments were performed by centrifugation at 181 000*g* (52 000 rpm) for absorbance at 280 nm after incubation of the sample for 5 min at 27 000*g* (20 000 rpm). The protein boundary curves were detected at 6-min intervals.

Seeding Reactions. Acid-unfolded β2-m at 0.2 mg/mL in the polymerizing buffer was incubated at 20 or 37 °C with the seed fibrils (final concentration: 0, 0.5, or 5.0 μg/mL). Aliquots of the sample were withdrawn at different time points, and the light scattering intensity of the solution was measured at 20 °C with a fluorescence spectrometer (Hitachi F-4500). All the measurements were performed using the polymerizing buffer at pH 2.5, except where otherwise specified.

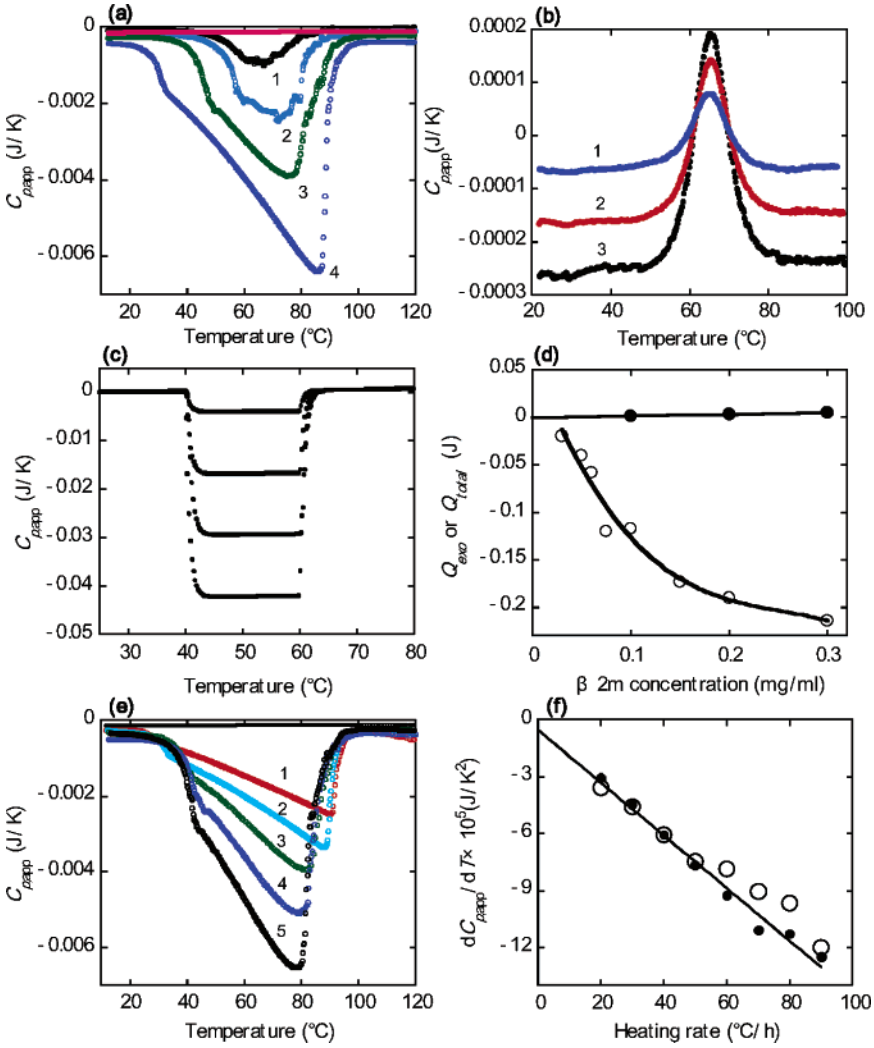

FIGURE 1: Thermal response associated with the formation of β2-m in a heat-induced state at pH 2.5. (a) DSC thermograms corresponding to the formation and disruption of the heat-induced state. The sample solution contained β2-m and 0.5 μg/mL seed fibrils, in which the β2-m concentrations (mg/mL) were varied: 1, 0.03; 2, 0.06; 3, 0.10; and 4, 0.30. The heating rate was 60 °C/h. The flat line represents the thermogram for 0.1 mg/mL β2-m without the seed fibrils. (b) DSC thermograms corresponding to the thermal-induced unfolding of β2-m in phosphate buffer at pH 7. The protein concentrations (mg/mL) were varied: 1, 0.10; 2, 0.20; and 3, 0.30. The heating rate was 60 °C/h. (c) Calibration marks by a known power pulse. Several calibration marks were obtained by input of a known power into one of the two cells. (d) Integrated heat (Q_{exo}) for the exothermic process in the heat-induced state. The Q_{exo} values were estimated from the area for the exothermic reaction as shown in panel a using Origin software and plotted as negative values, in which the flat $C_{p,app}$ trace before the transition and that released at high temperatures were used as baselines. The total heat (Q_{total}) for the thermal unfolding of β2-m was similarly estimated using the DSC thermograms in panel b and plotted as positive values. (e) Heating rate-dependent exothermic processes in the heat-induced state. The heating rate (°C/h) was varied: 1, 20; 2, 30; 3, 50; 4, 70, and 5, 90. The sample solution contained 0.2 mg/mL β2-m and 0.5 μg/mL seed fibrils. The flat line represents the thermogram for the second heating after the first heating to 120 °C at 60 °C/h. (f) Heating rate-dependent $dC_{p,app}/dT$ at 60 °C corresponding to the thermal response of β2-m in the heat-induced state. The $dC_{p,app}/dT$ values were calculated from the slope of the linear temperature dependence from 58.5 to 61.5 °C of the $C_{p,app}$ traces obtained at various heating rates as shown in panel e. The β2-m concentrations were 0.1 (○) and 0.2 mg/mL (●). The solid line is the linear best fit to the data obtained at 0.2 mg/mL β2-m.

RESULTS

Unique Thermal Response of the Acid-Unfolded β2-m in the Presence of Seed Fibrils. To characterize the effect of heat on the initial stages in the formation of amyloid fibrils, DSC measurements were performed, in which the temperature of a freshly mixed solution of acid-unfolded β2-m (various concentrations) and seed fibrils (0.5 μg/mL) was increased at 60 °C/h (Figure 1a). In the absence of seed fibrils, no effect of heat was observed, and the apparent heat capacity ($C_{p,app}$) of the acid-unfolded β2-m solution, which is slightly smaller than that of the buffer solution, was retained. However, the addition of seed fibrils produced unique $C_{p,app}$ traces characterized by a sigmoidal transition: an abrupt decrease in $C_{p,app}$ followed by a relatively linear decrease at around 30∼50 °C. As the protein concentration increased, the transition temperature dropped and the amplitude of the change in $C_{p,app}$ increased. After the linear decrease, the $C_{p,app}$ increased markedly to a value close to zero at 70∼100 °C.

The $C_{p,app}$ traces were irreversible; the DSC thermogram for the second heating of the sample after cooling from the first heating to 120 °C showed no unique trace, and corresponded to that of the acid unfolded β2-m (Figure 1e), indicating that the heat-induced state produced by the first scan in the presence of the seed fibrils disintegrated with the heating to 120 °C. Since the fibril growth of β2-m is

accelerated up to 60 °C (*9*), it is likely that the DSC thermograms include heat associated with the formation and subsequent reaction of fibrils. Here, we try to address the underlying conformational changes leading to the unique DSC thermograms.

To compare the observed heat flow with that of protein unfolding, the thermal unfolding of the native β2-m at pH 7 was recorded. The unfolding proceeded with a single heat absorption peak typical of small globular proteins (Figure 1b). Notably, the effect of heat observed for the acid-unfolded β2-m in the presence of seed fibrils is much larger in magnitude than that for the unfolding of the native fold. To confirm the validity of the measurements, several calibration marks were recorded by inputting a known power into one of the two cells (Figure 1c), showing that the observed exothermal heat flow is within the instrumental capacity.

The integrated heat (Q_{exo}) associated with the exothermic process, which includes the heat for the formation of the heat-induced state, was estimated from the $C_{p,app}$ curves as shown in Figure 1a by using Origin software (Microcal, Inc.) and plotted as a function of the β2-m concentration (Figure 1d). We also plotted the total heat (Q_{total}) associated with the thermal unfolding of β2-m, corresponding to the enthalpy change of unfolding, multiplied by the protein concentration. When compared with the Q_{total} values, we detected more substantial heat flow for the heat-treatment of β2-m in the presence of seed fibrils.

The $C_{p,app}$ traces of acid-unfolded β2-m at 0.2 mg/mL in the presence of seed fibrils were recorded at the various heating rates (Figure 1e). Intriguingly, the thermal response was definitely dependent on the heating rate; namely, the $C_{p,app}$ value after the sigmoidal transition became more negative with the increase in the heating rate. The melting temperature decreased slightly with the increase in the heating rate. The temperature-dependence of $C_{p,app}$ (i.e., $dC_{p,app}/dT$) at 60 °C after the transition was estimated from these $C_{p,app}$ traces and plotted as a function of the heating rate (Figure 1f), revealing a linear dependence on the heating rate. We also performed the same experiments at 0.1 mg/mL β2-m and obtained very similar results as those shown in Figure 1e (data not shown). As a result, the dependence of $dC_{p,app}/dT$ at 60 °C on the heating rate was almost the same at the two β2-m concentrations, 0.1 and 0.2 mg/mL (Figure 1f), indicating a kinetic thermal response far removed from thermodynamic equilibrium.

Thermal Response of the Mature Amyloid Fibrils. The kinetic thermal response observed here shares clear similarity with the thermal response of mature β2-m amyloid fibrils (*35*). To compare exactly the thermal responses of the two conformational states, we repeated the experiments with the mature amyloid fibrils; DSC thermograms of mature β2-m amyloid fibrils that formed in the presence of 5.0 μg/mL seed fibrils at 37 °C overnight,were recorded (Figure 2a). Consistent with the previous paper (*35*), there was a remarkably large decrease in the $C_{p,app}$ as the temperature increased, followed by an abrupt increase at around 75−95 °C, showing the transformation in structure of the amyloid fibril to the unfolded state. The minimum peak in the DSC curves of amyloid fibrils corresponds to the temperature at which the thermal unfolding of the fibrils begins (*35*). Notably, since the temperature-dependence of $C_{p,app}$ becomes saturated at a fibril concentration above 0.04 mg/mL (*35*),

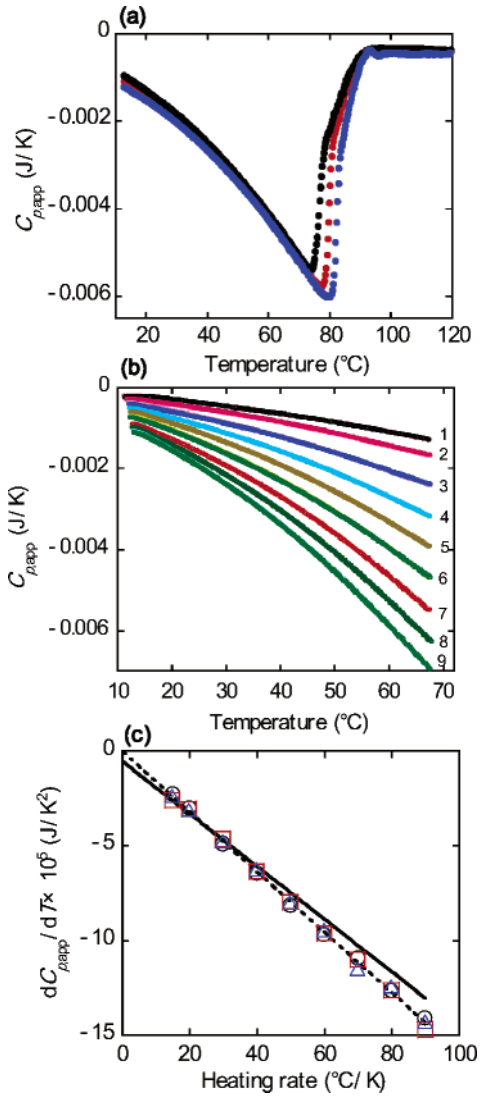

FIGURE 2: Thermal response of mature β2-m amyloid fibrils at pH 2.5. (a) DSC thermograms of mature β2-m amyloid fibrils in solution. The mature β2-m amyloid fibrils were formed by an extension reaction with 5 μg/mL seed fibrils at 37 °C overnight, in which the fibril concentrations were varied: black circles, 0.1; red circles, 0.2; and blue circles, 0.3 mg/mL. The heating rate was 60 °C/h. (b) The reversibility of DSC thermograms from 10 to 68 °C at the various heating rates. The fibril concentrations were 0.2 mg/mL. Heating was performed twice at each heating rate (°C/h): 1, 15; 2, 20; 3, 30; 4, 40; 5, 50; 6, 60; 7, 70; 8, 80; and 9, 90. (c) Heating rate dependence of $dC_{p,app}/dT$ values at 60 °C. $dC_{p,app}/dT$ was evaluated in the temperature range of 58.5 to 61.5 °C from the linear slope of the $C_{p,app}$ traces obtained at the various heating rates. The fibril concentrations were 0.1 (○), 0.2 (□), and 0.3 mg/mL (△). The dotted line is the linear best fit to the data obtained at 0.2 mg/mL fibrils. The solid line is the same as that in Figure 1f.

the $C_{p,app}$ traces recorded at relatively high fibril concentrations, 0.1, 0.2, and 0.3 mg/mL, showed almost the same temperature-dependence before the unfolding (Figure 2a).

In contrast to the unfolding transition, the DSC thermograms prior to the unfolding of fibrils (i.e., the minimum peak) were completely reversible as confirmed by the reheating runs at various heating rates at 0.2 mg/mL (Figure 2b). As reported previously, the $C_{p,app}$ values at 20 and 67 °C obtained from the traces in Figure 2b linearly depended on the heating rate and corresponded to those of the acid-unfolded form at the zero heating rate within the heat range

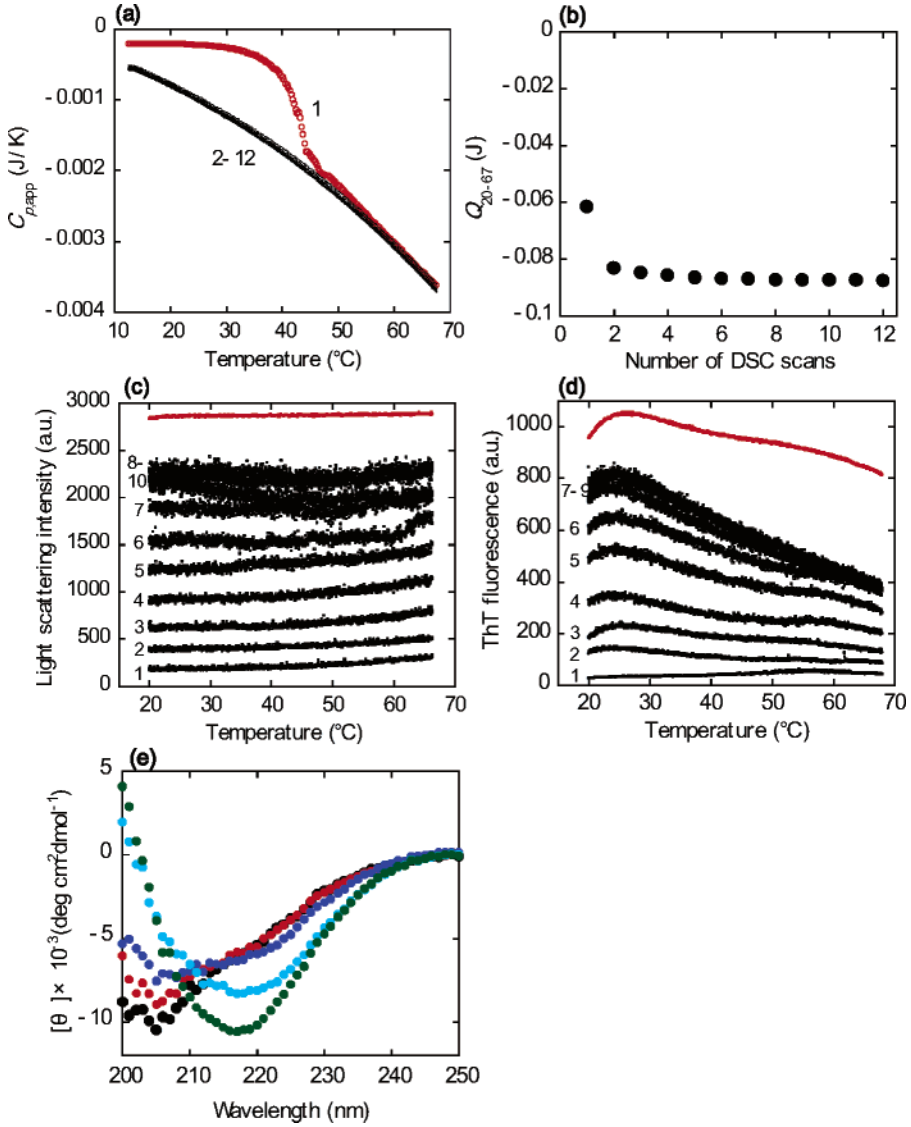

FIGURE 3: Growth of the heat-induced conformation during repeated heating at pH 2.5. The sample solution contained 0.2 mg/mL β2-m and 0.5 μg/mL seed fibrils. (a) DSC thermograms obtained in the repeated DSC scans. The scans were consecutively performed 12 times at 60 °C/h. The numbers 1−12 correspond to the number of scans. (b) Integrated heat (Q_{20-67}) for the exothermic reaction against the number of DSC scans. The Q_{20-67} values were estimated over 20−67 °C from the area for the exothermic reaction using Origin software and plotted as negative values, in which the $C_{p,app}$ trace prior to the transition was drawn horizontally to a higher temperature range and used as a baseline. (c and d) Changes in light scattering (c) and ThT fluorescence (d) intensities during the heating−cooling−reheating cycles. The temperature was increased from 20 to 68 °C at 60 °C/h, and the sample solutions were mildly agitated during the heating to prevent the sedimentation of fibrils. The numbers 1−10 correspond to the number of heat treatments. Red lines represent the data for amyloid fibrils from the same sample incubated at 37 °C overnight. The final concentration of ThT was 10 μM. (e) Changes in far-UV CD spectra at 20 °C after repeated heating−cooling−reheating. The sample was repeatedly heated from 20 to 68 °C at 60 °C/h without agitation. Black circles, the sample before heating; red circles, after the first heating; blue circles, after the fourth heating; light blue circles, after the eighth heating; and green circles, amyloid fibrils formed by the incubation at 37 °C overnight with the same sample solution.

presented (data not shown, see Figure 3b of ref 35). The $dC_{p,app}/dT$ value at 60 °C was estimated using the data in Figure 2b and plotted against the various heating rates, along with that obtained in the heat-induced state (Figure 2c). Importantly, this plot for the mature amyloid fibrils was very similar to that for the heat-induced conformation starting with the acid-unfolded β2-m in the presence of seed fibrils, implying that the heat treatment indeed produced a significant amount of mature fibrils. However, this was not the case as will be described below.

Growth of Amyloid Fibrils during Repeated Heating. To clarify the difference between the heat-induced conformation and the mature amyloid fibrils, repeated DSC thermograms of the solution containing 0.2 mg/mL of β2-m and 0.5 μg/mL of seed fibrils were recorded, in which heating−cooling−reheating prior to the unfolding of fibrils was performed 12 times in a row (Figure 3a). After a sigmoidal curve corresponding to the formation of the heat-induced state observed for the first heating scan, almost the same $C_{p,app}$ traces were obtained during subsequent heating scans. The heat, Q_{20-67}, needed for the exothermic process was estimated over 20−67 °C from the $C_{p,app}$ traces and was plotted against the number of heating cycles (Figure 3b). The Q_{20-67} values were saturated after the first scan, further implying that a significant amount of fibrils was produced by the first heating scan.

Then, light scattering, ThT fluorescence, and far-UV CD were used to directly monitor the formation of fibrils during

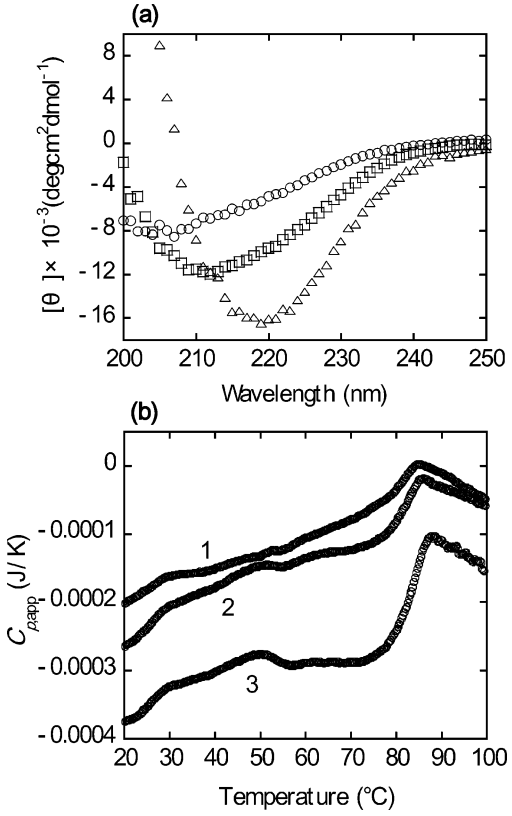

FIGURE 4: Secondary structure and thermal response of salt-induced β2-m protofibrils at pH 2.5. (a) Far-UV CD spectra of salt-induced protofibrils (□), mature amyloid fibrils (△), and β2-m in the acid-unfolded state (○), in which the β2-m concentrations were 0.2 mg/mL. (b) DSC thermograms of salt-induced protofibrils, in which the fibril concentrations (mg/mL) were varied: 1, 0.2; 2, 0.3; and 3, 0.5. The heating rate was 60 °C/h.

the repeated heating, for which the solvent and protein concentration were the same as for the DSC measurements. Contrary to our expectation given the effects of heat (Figure 3a,b), the first heating did not produce a notable amount of amyloid fibrils (Figure 3c−e). Instead, the changes in light scattering intensity, ThT fluorescence, and the far-UV CD spectrum indicated gradual growth accompanied by an increase in β-sheet content with a minimum at around 218 nm that is typical for mature amyloid fibrils (see Figure 4a). However, the saturated maximum values of light scattering, ThT fluorescence, and far-UV CD intensity were less than those of amyloid fibrils formed by the extension reaction at 37 °C from the same sample. In addition, significant perturbation of light scattering and ThT fluorescence was observed as the number of heating cycles increased, in comparison with those of the amyloid fibrils formed at 37 °C. These results suggest that repeated heating also induced the aggregation of amyloid fibrils.

Thermal Response of the Salt-Induced Fibrils. Since a thermal response very similar to that of mature amyloid fibrils was observed for the heat-treated β2-m even in the absence of a significant amount of fibrils, it may be that various conformational states exhibit a kinetic thermal response as shown here. Therefore, we examined the thermal response of the salt-induced "Protofibrils" of β2-m that formed spontaneously at pH 2.5 in the presence of 0.5 M NaCl without seed fibrils. The salt-induced protofibrils are seemingly flexible and nodular in appearance in contrast to the long, straight mature amyloid fibrils (*17*). The far-UV CD spectrum of the salt-induced fibrils is characterized by a negative peak at around 212 nm, which is different from that of the mature amyloid fibrils which have a negative peak at around 219 nm (Figure 4a). The resultant $C_{p,app}$ traces of the salt-induced fibrils revealed an endothermic peak at around 70−100 °C corresponding to the unfolding of protofibrils (Figure 4b). Notably, no large decrease in $C_{p,app}$ before the unfolding was observed for the salt-induced protofibrils, indicating that the kinetic thermal response is unique to particular type(s) of fibrils.

AFM Measurements. AFM images were examined to characterize the heat-induced state of β2-m (Figure 5). The freshly mixed solution of 0.2 mg/mL β2-m and 0.5 μg/mL seed fibrils showed no noticeable aggregates, except for dots probably representing the seed fibrils (Figure 5a). Incubation of the same sample overnight at 37 °C produced amyloid fibrils that were long and straight (Figure 5b). Here, the heat-induced state of the same sample, which was heated to 68 °C at 60 °C/h and cooled, revealed the presence of amyloid fibrils (Figure 5c). However, the amount generated upon the single heating scan appeared to be small, consistent with the low level of light scattering (Figure 3c). The incubation of this small amount overnight at 37 °C produced a large amount of fibrils, indicating that the fibrils produced by the heat treatment further propagated by incorporating the monomers (Figure 5d).

Ultracentrifugation Measurements. To further characterize the fibrils formed after the first heating scan, we measured the sedimentation velocity at pH 2.5, in which three different samples were used: a solution of 0.2 mg/mL of β2-m monomer, a mixture containing 0.2 mg/mL of the monomer and 0.5 μg/mL of seed fibrils, and the same mixture subjected to heat treatment up to 68 °C at 60 °C/h and cooling. The spinning was conducted in two steps: at 27 000*g* and subsequently at 181 000*g*. The movements of the boundary of these samples during the spinning at 181 000*g* were recorded (Figure 6a−c), showing that the boundary broadened by diffusion. It is important to note that the concentration at the plateau of the initial boundary movements (i.e., maximum absorbance at 280 nm) for the heat-treated sample was lower by 12% than that for the other two samples. This decrease in absorbance could be attributed to the rapid sedimentation of the fibrils formed by the heat treatment during the spinning at 27 000*g*. For the three samples, an analysis of the sedimentation pattern in Figure 6a−c showed little significant difference for the association of the protein molecules (Figure 6d). Thus, the heat-treated sample mainly consists of two components: acid-unfolded monomers and fibrils separated sharply at 27 000*g*. These fibrils were too large to estimate a sedimentation coefficient, consistent with the observations by AFM. Consequently, the analysis of the sedimentation velocity suggests that the kinetic thermal response of the heat-induced conformation is attributed to the fibrils accounting for about 12% of all the β2-m molecules.

Seed-Dependent Extension Reaction. We then investigated the seed-dependent extension reaction to obtain some insight into the time-dependent kinetics for the fibrils formed by the heat treatment up to 68 °C. First, the seed-dependent fibril extension reactions of β2-m at 20 and 37 °C were monitored by light scattering, in which the concentrations of seed fibrils were varied, 0, 0.5, and 5 μg/mL (Figure 7).

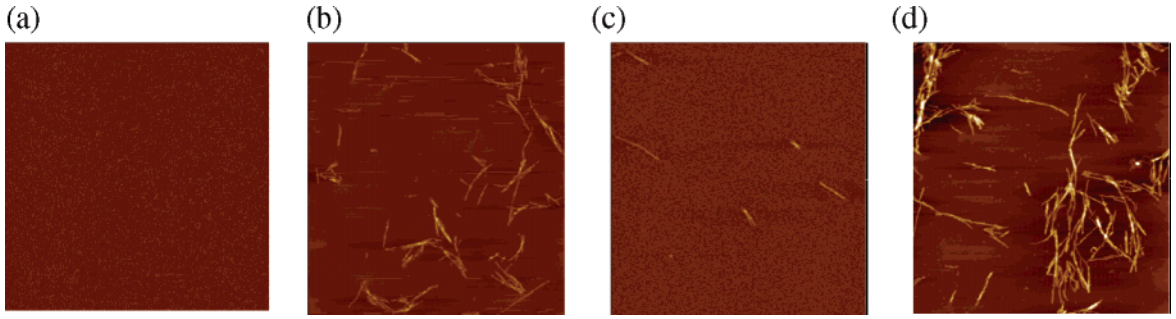

FIGURE 5: AFM images of the heat-induced form and amyloid fibrils. (a) Freshly mixed sample solution of 0.2 mg/mL β2-m and 0.5 μg/mL seed fibrils. (b) Amyloid fibrils formed by incubation at 37 °C overnight of the sample in panel a. (c) Heat-induced state, where the sample in panel a was heated to 68 °C at 60 °C/h and cooled. (d) Amyloid fibrils formed by the incubation at 37 °C overnight of the sample in panel c. All the sample solutions were diluted 5-fold with water before the measurement. The images are by 5 × 5 μm.

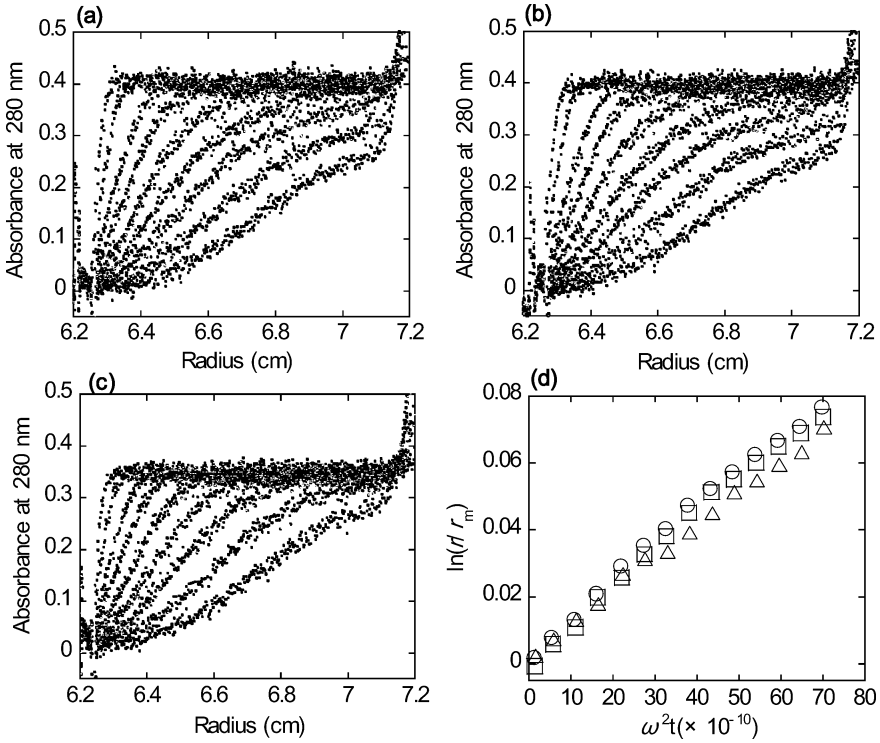

FIGURE 6: Ultracentrifuge-based analysis of three β2-m samples (0.2 mg/mL) at 4 °C and pH 2.5. (a−c) Representative sedimentation profiles: (a) β2-m solution without the seed fibrils, (b) β2-m solution with 0.5 μg/mL seed fibrils, (c) the heat-treated sample; the sample was the same as in panel b, but heated from 20 to 68 °C at 60 °C/h and cooled to 4 °C. The three sedimentation patterns were recorded at the same time intervals for the absorbance at 280 nm. (d) Analysis of the sedimentation patterns. The $\ln(r/r_m)$ versus $\omega^2 t$ plot for the three samples used, ○, (a); □, (b), and △, (c), where r_m is the radial position of the meniscus, r is the midpoint position of the boundaries, t is time in seconds, and ω is the angular velocity.

When 0.2 mg/mL of β2-m and 5 μg/mL of seed were incubated, a significant increase in the light scattering intensity was observed without a lag time at the two temperatures. In the presence of 0.5 μg/mL of seed fibrils, however, the extension reaction was relatively slow with a lag time, resulting in a characteristic sigmoidal time course. No fibrils were detected in the monomeric protein solution without the seed fibrils by light scattering.

Next, after the freshly mixed solution of β2-m at 0.2 mg/mL and seed fibrils at 0.5 μg/mL was heated from 20 to 68 °C at 60 °C/h and immediately cooled, the extension reaction of this sample solution was monitored by light scattering at both 20 and 37 °C (Figure 7). This heat-treated sample exhibited a marked increase in light scattering without a lag time from a relatively high value. This high level of light scattering suggests a slight increase in the amount of fibrils, which was produced by the seed-dependent growth during the heat treatment. In fact, at both 20 and 37 °C, the time course of the extension reaction for the heat-treated sample is similar to that after the lag phase without the heat treatment.

DISCUSSION

Kinetically Controlled Thermal Response of Amyloid Fibrils. DSC, a direct and powerful technique for evaluating the amount of heat associated with a biophysical process, particularly protein unfolding, has also revealed the unique exothermic process associated with tubulin polymerization and protein aggregation (*36*, *37*). However, the formation of protein aggregates has a profound effect on the DSC curves, precluding their use established for analyzing equilibrium thermodynamics (*38*). Previously, we reported unique thermal responses of amyloid fibrils suggesting that the hydration patterns of these fibrils are distinct from those of

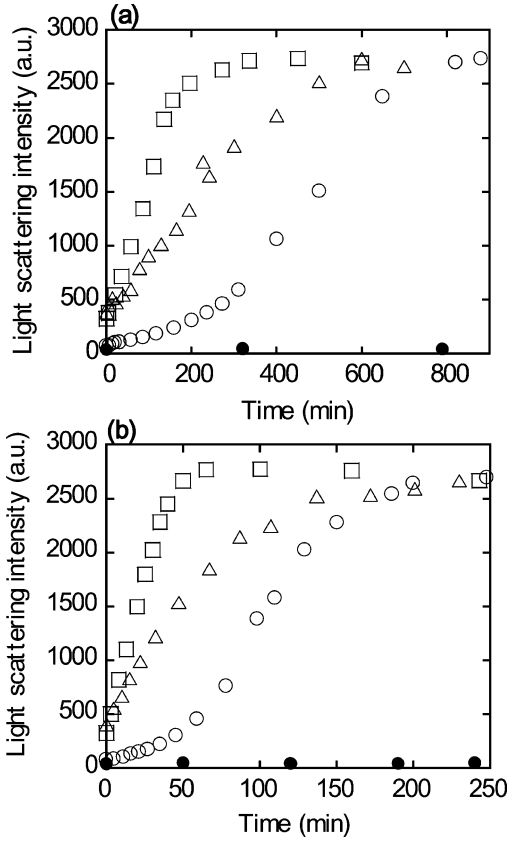

FIGURE 7: Seeding-dependent amyloid fibril growth monitored by light scattering at pH 2.5 and 20 (a) or 37 (b) °C. The reaction solution contained β2-m at 0.2 mg/mL and seed fibrils at different concentrations. ●, 0 μg/mL seeds; ○, 0.5 μg/mL seeds; □, 5.0 μg/mL seeds; Δ, heat-treated sample with 0.5 μg/mL seed fibrils; after the freshly mixed solution of β2-m and 0.5 μg/mL seeds was heated to 68 °C at 60 °C/h and cooled, the extension reaction of the heat-treated sample was monitored.

globular proteins and that the observed change in heat capacity is predominantly determined by the solvent (*35*). We notice that the thermal response of amyloid fibrils reported previously (*35*) resembles that of tubulin polymerization (*36*). Considering that amyloid fibrils are a generic structure common to various proteins, studying systems which do not satisfy the calorimetric criterion established with small globular proteins is becoming increasingly important. In the present study, we observed an exothermic heat response accompanied by a sigmoidal transition when the monomeric β2-m was heated in the presence of a small amount of seed fibrils. The kinetic thermal response after the sigmodal transition was practically the same as that of the mature β2-m amyloid fibrils (*35*). We believe that the observed unique effects of heat provide important clues to understanding the calorimetric properties and moreover the structural stability of amyloid fibrils.

Since the rate of fibril growth increases with an increase in temperature up to about 60 °C (*9*), we first assumed that the observed effects of heat are coupled with the conversion of most of the β2-m molecules into amyloid fibrils. However, a structural analysis of the heat-treated samples using various methods including light scattering, ThT fluorescence, CD, AFM, and ultracentrifugation measurements excluded this possibility. Instead, the amount of fibrils formed by the first heat treatment at 0.2 mg/mL β2m in the presence of seed fibrils at 0.5 μg/mL is only about 12% as monitored with sedimentation velocity measurements. Considering the result of ultracentrifugation, that the remaining 88% stays monomeric, conformational states other than unfolded monomers and fibrils are unlikely to play a role in the unique response of heat.

So, can the conversion of 12% (0.024 mg/mL) of β2-m molecules (0.2 mg/mL) into amyloid fibrils during the heating scan explain the kinetic thermal response observed for the solution of mature amyloid fibrils? A previous paper has shown that the temperature dependence of $C_{p,app}$ associated with the exothermic process becomes saturated above a certain concentration of the fibrils (i.e., 0.04 mg/mL) (*35*). In fact, as shown in Figure 2c, the slopes of $dC_{p,app}/dT$ versus the heating rate for the mature amyloid fibrils were independent of the fibril concentration of 0.1−0.3 mg/mL. Therefore, a small amount of fibril produced during the heat treatment may reproduce the unique calorimetric property observed for the solution of mature fibrils, although the amount of these fibrils (∼0.024 mg/mL) is smaller than the value of 0.04 mg/mL.

While the Q_{20-67} values detected by the repeated DSC scans were almost saturated after the sigmoidal transition in the first heating, the fibrils continued to grow during the repeated scans (Figure 3). Although the exothermic heat identifying the fibril extension reaction is expected to occur during the DSC heating cycles, this reactive heat at a constant temperature under the conditions used was found to be markedly lower than the enthalpy changes of thermal-induced unfolding of β2-m (*27*). Additionally, it should be noted that the mature amyloid fibrils, where the fibril elongation is completed, have shown a very similar thermal response to that of the partly formed amyloid fibrils (Figure 2c). These results strongly suggest that the saturated Q_{20-67} values (i.e., exothermic effect) can be ascribed to the kinetic thermal response arising from the presence of the partly formed amyloid fibrils, rather than the heat from fibril elongation. Thus, it follows that the same kinetic effect occurs despite the structural evolution from the partially formed fibrils to the fully formed mature amyloid fibrils.

Then, what kinds of structural properties are responsible for the sigmoidal transition leading to the remarkably decreased $C_{p,app}$ value, which decreases even further and linearly with an increase in temperature? The heat detected by scanning calorimetry is attributed to the partial specific heat capacities of solutes, solvents, or both related to the solvent−solute interactions. The $C_{p,app}$ values of the amyloid fibril solution are extrapolated at a zero heating rate to that of unfolded protein, suggesting that the $C_{p,app}$ values of amyloid fibrils and its precursor proteins are indistinguishable at equilibrium within the heat scale presented. Consequently, the heating rate-dependent, largely negative $C_{p,app}$ value is assumed to be caused by a dynamic interaction between the solvent and protein that is probably sensitive to the specific β-structure in the aggregates or fibrils. Accordingly, it is conceivable that the property of protein−water varies significantly at the point where the $C_{p,app}$ sharply decreases (i.e., sigmoidal transition), where fibril growth exceeds some limiting point.

Although a clear-cut explanation is not given for the origin of the kinetic control observed in this and the previous study (*35*), we would suggest that the large heating rate-dependent decrease in $C_{p,app}$ is induced by a transient organization of

the fibril−water network that reduces the surface area of polymerized fibrils or aggregates that is accessible to the solvent and produces more motionless water molecules with a lower heat capacity (*39*, *40*). Furthermore, the unique calorimetric property of the mature amyloid fibrils may be coupled to a specific hydration pattern. The amyloid fibrils structure is organized by cross-β-sheets with the side chain packing in a different manner from that of the native fold (*4*−*7*). Hydrophobic effects through protein−water interactions (i.e., hydrophobic hydration) is perhaps the major driving force of the fibrillation as well as the native folding. In both cases, the overall energetics including the enthalpy change is determined by a balance between various intramolecular and intermolecular interactions, some favoring the amyloid or folded states and some favoring the unfolded state (*6*, *25*, *41*). Thus, it is also possible that the characteristic exothermic heat observed with amyloid fibrils represents the loss of compensation of opposing large contributions.

Exothermic Thermal Response Is Not Necessarily Common to Fibrillar Structures. In the amyloid fibril formation of several proteins, a hierarchical mechanism has been proposed, in which protofibrils with a flexible morphology are an intermediate of the long-straight, well-ordered fibrils (*3*). On the other hand, it has been reported that the formation of amyloid fibrils of β2m at low pH (2.5−3.5) in vitro occurs via at least two parallel extension routes based on a careful choice of salt concentrations (*25*, *29*, *42*). The first route occurs at low concentrations of salt through a nucleation-growth mechanism involving a lag time, producing needlelike and well-ordered fibrils (i.e., mature amyloid fibrils). In this case, the addition of seed fibrils would generally reveal a rapid extension reaction without a lag time, consistent with the limiting nucleation phase being bypassed. The experimental conditions of pH 2.5 and 0.1 M NaCl used in this study lead to this route of fibril assembly (Figure 7). In contrast, at the same pH and high salt concentrations, curved and flexible fibrils are spontaneously formed, corresponding to the salt-induced protofibrils used in this study. Since no transformation from the salt-induced protofibrils to the mature fibrils was observed in previous studies, the salt-induced protofibrils are considered to be another type of fibril: a dead-end product of fibrillation (*17*, *25*, *29*, *42*). The result that the salt-induced protofibrils did not show a kinetic thermal response supports the idea that the two types of fibril structure are not compatible with each other.

The salt-induced protofibrils are assumed to have relatively heterogeneous intermolecular interactions with a lower propensity to bind thioflavin-T (*25*). A distinctive feature of the salt-induced formation of fibrils is that it does not require the formation of a critical nucleus. Such nonnuclear fibril formation was observed in the self-assembly of other proteins and peptides and interpreted in terms of the colloid coagulation theory (*11*, *12*). The salt-induced protofibrils of β2-m revealed an endothermic peak corresponding to the unfolding of fibrils. Similar effects of heat on the DSC data have been observed elsewhere (*43*−*45*). On the other hand, the fibrils formed after the sigmoidal transition and the mature amyloid fibrils of β2-m exhibited an exothermic heat effect prior to their thermal unfolding. In this case, the endothermic heat for the dissociation of fibrils or aggregates may be behind the enormous heat flow accompanied by the disappearance of the exothermic heat effect.

In conclusion, although an exact structural and calorimetric interpretation of the tremendously large effects of heat as observed previously for the β2-m amyloid fibrils remains to be made, the present results demonstrated that unique thermal effects can be induced during the DSC scan of β2-m monomers coupled with seed-dependent fibril growth. These effects were totally absent in the salt-induced protofibrils, probably representing a less or differently organized structure with respect to the hydration or trapped water molecules. Thus, analysis with DSC will be useful to estimate the extent of the organization and hydration of amyloid fibrils and other aggregates.

ACKNOWLEDGMENT

We thank Miyo Sakai (Institute for Protein Research) for conducting the analytical ultracentrifugation experiments.

REFERENCES

1. Kelly, J. W. (1998) The alternative conformations of amyloidogenic proteins and their multi-step assembly pathways, *Curr. Opin. Struct. Biol. 8*, 101−106.
2. Dobson, C. M. (2003) Protein folding and misfolding, *Nature 426*, 884−890.
3. Ross, C. A., and Poirier, M. A. (2004) Protein aggregation and neurodegenerative disease, *Nat. Med. 10*, s10−s17.
4. Tycko, R. (2004) Progress towards a molecular-level structural understanding of amyloid fibrils, *Curr. Opin. Struct. Biol. 14*, 96−103.
5. Fändrich, M., and Dobson, C. M. (2002) The behaviour of polyamino acids reveals an inverse side chain effect in amyloid structure formation, *EMBO J. 21*, 5682−5690.
6. Saiki, M., Honda, S., Kawasaki, K., Zhou, D., Kaito, A., Konakahara, T., and Morii, H. (2005) Higher-order molecular packing in amyloid-like fibrils constructed with linear arrangements of hydrophobic and hydrogen-bonding side-chains, *J. Mol. Biol. 348*, 983−998.
7. Makin, O. S., and Serpell, L. C. (2005) Structures for amyloid fibrils, *FEBS J. 272*, 5950−5961.
8. Harper, J. D., and Lansbury, P. T. Jr. (1997) Models of amyloid seeding in Alzheimer's disease and scrapie: mechanistic truths and physiological consequences of the time-dependent solubility of amyloid proteins, *Annu. Rev. Biochem. 66*, 385−407.
9. Naiki, H., Hashimoto, N., Suzuki, S., Kimura, H., Nakakuki, K., and Gejyo, F. (1997) Establishment of a kinetic model of dialysis-related amyloid fibril extension in vitro, *Amyloid 4*, 223−232.
10. Uversky, V. N., and Fink, A. L. (2004) Conformational constraints for amyloid fibrillation: the importance of being unfolded, *Biochim. Biophys. Acta 1698*, 131−153.
11. Modler, A. J., Gast, K., Lutsch, G., and Damaschun, G. (2003) Assembly of amyloid protofibrils via critical oligomers-a novel pathway of amyloid formation, *J. Mol. Biol. 325*, 135−148.
12. Carrotta, R., Manno, M., Bulone, D., Martorana, V., and San Biagio, P. L. (2005) Protofibril formation of amyloid β-protein at low pH via a non-cooperative elongation mechanism, *J. Biol. Chem. 280*, 30001−30008.
13. Bhattacharyya, A. M., Thakur, A. K., and Wetzel, R. (2005) Polyglutamine aggregation nucleation: thermodynamics of a highly unfavorable protein folding reaction, *Proc. Natl. Acad. Sci. U.S.A. 102*, 15400−15405.
14. Bader, R., Bamford, R., Zurdo, J., Luisi, B. F., and Dobson, C. M. (2006) Probing the mechanism of amyloidogenesis through a tandem repeat of the PI3-SH3 domain suggests a generic model for protein aggregation and fibril formation, *J. Mol. Biol. 356*, 189−208.
15. Bjorkman, P. J., Saper, M. A., Samraoui, B., Bennett, W. S., Strominger, J. L., and Wiley, D. C. (1987) Structure of the human class I histocompatibility antigen, HLA-A2, *Nature 329*, 506−512.
16. Yamamoto, S., and Gejyo, F. (2005) Historical background and clinical treatment of dialysis-related amyloidosis, *Biochim. Biophys. Acta 1753*, 4−10.

17. Hong, D.-P., Gozu, M., Hasegawa, K., Naiki, H., and Goto, Y. (2002) Conformation of β_2-microglobulin amyloid fibrils analyzed by reduction of the disulfide bond, *J. Biol. Chem. 277*, 21554−21560.
18. Hoshino, M., Katou, H., Hagihara, Y., Hasegawa, K., Naiki, H., and Goto, Y. (2002) Mapping the core of the β_2-microglobulin amyloid fibril by H/D exchange, *Nat. Struct. Biol. 9*, 332−336.
19. Kad, N. M., Myers, S. L., Smith, D. P., Alastair Smith, D., Radford, S. E., and Thomson, N. H. (2003) Hierarchical assembly of β_2-microglobulin amyloid in vitro revealed by atomic force microscopy, *J. Mol. Biol. 330*, 785−797.
20. Chiba, T., Hagihara, Y., Higurashi, T., Hasegawa, K., Naiki, H., and Goto, Y. (2003) Amyloid fibril formation in the context of full-length protein: effects of proline mutations on the amyloid fibril formation of β_2-microglobulin, *J. Boil. Chem. 278*, 47016−47024.
21. Ban, T., Hamada, D., Hasegawa, K., Naiki, H., and Goto, Y. (2003) Direct observation of amyloid fibril growth monitored by thioflavin T fluorescence, *J. Biol. Chem. 278*, 16462−16465.
22. Ohhashi, Y., Hasegawa, K., Naiki, H., and Goto, Y. (2004) Optimum amyloid fibril formation of a peptide fragment suggests the amyloidogenic preference of β_2-microglobulin under physiological conditions, *J. Biol. Chem. 279*, 10814−10821.
23. Yamaguchi, K., Takahashi, S., Kawai, T., Naiki, H., and Goto, Y. (2005) Seeding-dependent propagation and maturation of amyloid fibril conformation, *J. Mol. Biol. 352*, 952−960.
24. Wadai, H., Yamaguchi, K., Takahashi, S., Kanno, T., Kawai, T., Naiki, H., and Goto, Y. (2005) Stereospecific amyloid-like fibril formation by a peptide fragment of β_2-microglobulin, *Biochemistry 44*, 157−164.
25. Raman, B., Chatani, E., Kihara, M., Ban, T., Sakai, M., Hasegawa, K., Naiki, H., Rao, C. M., and Goto, Y. (2005) Critical balance of electrostatic and hydrophobic interactions is required for β_2-microglobulin amyloid fibril growth and stability, *Biochemistry 44*, 1288−1299.
26. Ivanova, M. I., Sawaya, M. R., Gingery, M., Attinger, A., and Eisenberg, D. (2004) An amyloid-forming segment of β2-microglobulin suggests a molecular model for the fibril, *Proc. Natl. Acad. Sci. U.S.A. 101*, 10584−10589.
27. Kardos, J., Yamamoto, K., Hasegawa, K., Naiki, H., and Goto, Y. (2004) Direct measurement of the thermodynamic parameters of amyloid formation by isothermal titration calorimetry, *J. Biol. Chem. 279*, 55308−55314.
28. Chatani, E., Kato, M., Kawai, T., Naiki, H., and Goto, Y. (2005) Main-chain dominated amyloid structures demonstrated by the effect of high pressure, *J. Mol. Biol. 352*, 941−951.
29. Gosal, W. S., Morten, I. J., Hewitt, E. W., Smith, D. A., Thomson, N. H., and Radford, S. E. (2005) Competing pathways determine fibril morphology in the self-assembly of β_2-microglobulin into amyloid, *J. Mol. Biol. 351*, 850−864.
30. Balbirnie, M., Grothe, R., and Eisenberg, D. S. (2001) An amyloid-forming peptide from the yeast prion Sup35 reveals a dehydrated β-sheet structure for amyloid, *Proc. Natl. Acad. Sci. U.S.A. 98*, 2375−2380.
31. Perutz, M. F., Finch, J. T., Berriman, J., and Lesk, A. (2002) Amyloid fibers are water-filled nanotubes, *Proc. Natl. Acad. Sci. U.S.A. 99*, 5591−5595.
32. Cordeiro, Y., Kraineva, J., Ravindra, R., Lima, L. M., Gomes, M. P. B., Foguel, D., Winter, R., and Silva, J. L. (2004) Hydration and packing effects on prion folding and β-sheet conversion. High-pressure spectroscopy and pressure perturbation calorimetry studies, *J. Biol. Chem. 279*, 32354−32359.
33. Broome, B. M., and Hecht, M. H. (2000) Nature disfavors sequences of alternating polar and non-polar amino acids: implications for amyloidogenesis, *J. Mol. Biol. 296*, 961−968.
34. Benyamini. H., Gunasekaran, K., Wolfson, H., and Nussinov, R. (2003) β_2-Microglobulin amyloidosis: insights from conservation analysis and fibril modelling by protein docking techniques, *J. Mol. Biol. 330*, 159−174.
35. Sasahara, K., Naiki, H., and Goto, Y. (2005) Kinetically controlled thermal response of β_2-microglobulin amyloid fibrils, *J. Mol. Biol. 352*, 700−711.
36. Berkowitz, S. A., Velicelebi, G., Sutherland, J. W. H., and Sturtevant, J. M. (1980) Observation of an exothermic process associated with the in vitro polymerization of brain tubulin, *Proc. Natl. Acad. Sci. U.S.A. 77*, 4425−4429.
37. Dzwolak, W., Ravindra, R., Lendermann, J., and Winter, R. (2003) Aggregation of bovine insulin probed by DSC/PPC calorimetry and FTIR spectroscopy, *Biochemistry 42*, 11347−11355.
38. Weijers, M., Barneveld, P. A., Cohen Stuart, M. A., and Visschers, R. W. (2003) Heat-induced denaturation and aggregation of ovalbumin at neutral pH described by irreversible first-order kinetics, *Protein Sci. 12*, 2693−2703.
39. Stites, W. E. (1997) Protein−protein interactions: interface structure, binding thermodynamics, and mutational analysis, *Chem. Rev. 97*, 1233−1250.
40. Bergqvist, S., Williams, M. A., O'Brien, R., and Ladbury, J. E. (2004) Heat capacity effects of water molecules and ions at protein-DNA interface, *J. Mol. Biol. 336*, 829−842.
41. Dill, K. A. (1990) Dominant forces in protein folding, *Biochemistry 29*, 7133−7155.
42. Radford, S. E., Gosal, W. S., and Platt, G. W. (2005) Towards an understanding of the structural molecular mechanism of β_2-microglobulin amyloid formation in vitro, *Biochim. Biophys. Acta 1753*, 51−63.
43. Azuaga, A. I., Dobson, C. M., Mateo, P. L., and Conejero-Lara, F. (2002) Unfolding and aggregation during the thermal denaturation of streptokinase, *Eur. J. Biochem. 269*, 4121−4133.
44. Rezaei, H., Choiset, Y., Eghiaian, F., Treguer, E., Mentre, P., Debey, P., Grosclaude, J., and Haertle, T. (2002) Amyloidogenic unfolding intermediates differentiate sheep prion protein variants, *J. Mol. Biol. 322*, 799−814.
45. Morel, B., Casares, S., and Conejero-Lara, F. (2006) A single mutation induces amyloid aggregation in the α-spectrin SH3 domain: analysis of the early stages of fibril formation, *J. Mol. Biol. 356*, 453−468.

BI0606748